*SF2A 2008*
*C. Charbonnel, F. Combes and R. Samadi (eds)*

# PULSATIONS OF RAPIDLY ROTATING STELLAR MODELS BASED ON THE SELF-CONSISTENT-FIELD METHOD: NUMERICAL ASPECTS AND ACCURACY

Reese, D.[1], MacGregor, K. B.[2], Jackson, S.[2], Skumanich, A.[2] and Metcalfe, T. S.[2]

**Abstract.** We use the numerical method developed in Lignières et al. (2006) and Reese et al. (2006) to calculate pulsation modes in stellar models generated by the Self-Consistent-Field method described in Jackson et al. (2005) and MacGregor et al. (2007). A discussion on the numerical method and its accuracy is given, followed by a very brief description of some of the results.

## 1 Introduction

Rapid stellar rotation introduces a number of phenomena which complicate stellar modelling. These include centrifugal deformation, gravity darkening, baroclinic flows and various forms of turbulence and transport phenomena (e.g. Rieutord 2006). As a result, the structure and evolution of these stars remain poorly understood and require observational constraints. Asteroseismology provides a promising way to probe the internal structure and dynamics of these stars, and thus to constrain stellar models.

Recent efforts to calculate stellar pulsations in rapidly rotating stars include Espinosa et al. (2004), Lignières et al. (2006), Reese et al. (2006), and Lovekin & Deupree (2008). These works either included a number of approximations, used a low resolution, or made use of simplified stellar models which limited the applicability of the results to actual observations. In the present paper, we use the numerical methods developed in Lignières et al. (2006) and Reese et al. (2006) to calculate the pulsation modes of stellar models based on the SCF method described in Jackson et al. (2005) and MacGregor et al. (2007), in an attempt to overcome these limitations.

## 2 The stellar models

The Self-Consistent-Field (SCF) method was first developed 40 years ago (Ostriker & Mark 1968). The basic idea in this method is to alternate between solving Poisson's equation, which gives the 2D shapes of the equipotentials, and solving the hydrostatic equation, which gives the 1D profile of thermodynamic quantities along a radial cut. This iterative procedure produces a series of models which converges to a rotating model which satisfies both equations. At the time, the method was restricted to massive stars due to what appeared to be numerical limitations. Since then these issues have been solved in a recent series of paper, and more realistic micro-physics have been included, thus allowing 1 or 2 $M_\odot$ models (Jackson et al. 2004, 2005; MacGregor et al. 2007).

Currently, models based on the SCF method are chemically homogeneous ZAMS models. The rotation profile is given by one of the following two equations:

$$\Omega(s) = \frac{\eta\Omega_{\rm cr}}{1+\left(\frac{\alpha s}{R_{\rm eq}}\right)^2} \qquad \text{or} \qquad \Omega(s) = \eta\Omega_{\rm cr}\left\{1+\left(\frac{\alpha s}{R_{\rm eq}}\right)^2\right\} \tag{2.1}$$

where $s$ is the distance to the rotation axis, $R_{\rm eq}$ the equatorial radius, $\Omega_{\rm cr}$ the equatorial break-up rotation rate, and $\alpha$ and $\eta$ two parameters which control the rotation profile. This type of rotation profile is conservative,

[1] Department of Applied Mathematics, University of Sheffield, Hicks Building, Hounsfield Road, Sheffield S3 7RH, UK
[2] High Altitude Observatory, National Center for Atmospheric Research, Boulder, CO 80307, USA

i.e. the centrifugal force derives from a potential. As a result, the stellar structure is barotropic: different thermodynamic quantities remain constant on surfaces of constant total potential, the sum of the centrifugal and gravitational potentials. Furthermore, the angular momentum $s^2\Omega$ increases with $s$, thus satisfying the dynamical part of the Solberg-Høiland stability criterion.

In the first type of rotation profile, the rotation rate decreases with increasing distance from the rotation axis. As a result, it is possible to construct configurations in which the central part rotates at an angular velocity which is several times $\Omega_{\rm cr}$. Such configurations can take on very distorted shapes and can be used to try to explain Achernar's oblateness (Jackson et al. 2004), as revealed by interferometric observations (Domiciano de Souza et al. 2003). In the second case, the rotation rate increases with distance to the rotation axis, thus partially resembling the solar rotation profile.

## 3 The stellar pulsations

Acoustic pulsation modes in the adiabatic approximation are governed by the following set of equations in an inertial frame:

$$[\lambda + im\Omega]\,\rho = -\vec{v}\cdot\vec{\nabla}\rho_0 - \rho_0\vec{\nabla}\cdot\vec{v}, \tag{3.1}$$

$$[\lambda + im\Omega]\,\rho_0\vec{v} = -\vec{\nabla}p + \frac{\vec{\nabla}P_0}{\rho_0}\rho - \rho_0\vec{\nabla}\Psi - 2\Omega\vec{e}_z\times\rho_0\vec{v} - \rho_0 s\frac{\partial\Omega}{\partial s}v_s\vec{e}_\phi \tag{3.2}$$

$$[\lambda + im\Omega]\,\left(p - c_0^2\rho\right) = \left[-\vec{\nabla}p_0 + c_0^2\vec{\nabla}\rho_0\right]\cdot\vec{v} \tag{3.3}$$

$$0 = \Delta\Psi - \Lambda\rho. \tag{3.4}$$

where $\vec{v}$ is the velocity perturbation, $\rho$ the Eulerian density perturbation, $p$ the Eulerian pressure perturbation, $\Psi$ the Eulerian perturbation to the gravitational perturbation, $\lambda = i\omega$ the eigenvalue (where $\omega$ is the eigenfrequency) and quantities with the subscript "0" equilibrium quantities. These equations are supplemented with boundary and regularity conditions which ensure that the pulsation modes are regular in the centre, the Lagrangian pressure perturbation vanishes on the stellar surface and the perturbation to the gravitational potential goes to zero towards infinity. The resultant system constitutes a 2D eigenvalue problem.

These equations are solved using the numerical method described in Lignières et al. (2006) and Reese et al. (2006). Firstly, an adapted coordinate system which follows the shape of the star is used. Rather than working with the equipotentials from the models, the same coordinate system is used as in Reese et al. (2006). This increases the accuracy of the geometrical terms which intervene in the equations, because the radial derivatives of $r$ are calculated analytically. An example of a coordinate system is shown in Fig. 1.

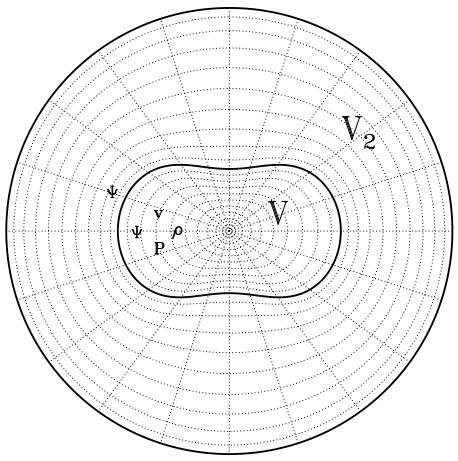


**Fig. 1.** An example of a coordinate system used when calculating pulsation modes. The inner domain, $V$, corresponds to the star. Equations (3.1)-(3.4) are solved on this domain, as represented by the symbols $\rho$, $P$, $\Psi$ and $\mathbf{v}$. In the second domain, $V_2$, only eq. (3.4) is solved, as represented by $\Psi$. This second domain is added in order to facilitate imposing the appropriate boundary conditions on the perturbation to the gravitational potential.

Secondly, the unknowns and the equations are projected onto the spherical harmonic basis. This is done by expressing the unknowns as a sum of spherical harmonics multiplied by unknown radial functions. The equations are multiplied by the complex conjugate of spherical harmonics and integrated over $4\pi$ steradians. The resultant system is an infinite set of coupled ordinary differential equations, the solution of which yields the

unknown radial functions. For numerical applications, this system is truncated at a maximal harmonic degree $L_{\max}$.

Finally, this system is discretised in the radial direction using $N_{\rm r}$ grid points thus yielding an algebraic system which can be solved using the Arnoldi-Chebyshev algorithm. This discretisation can be done using a spectral method based on Chebyshev polynomials as is done in Lignières et al. (2006) and Reese et al. (2006) or using finite differences as is the case here.

## 4 Accuracy of the results

Various tests can be used to assess the accuracy of the calculations. In Fig. 2, we follow the evolution of the error as a function of $L_{\max}$ and $N_{\rm r}$. The error was calculated by using the frequency calculated at highest resolution as a reference. The first two panels apply to a star rotating at 60% of the break-up rotation rate. As can be seen in the figure the accuracy is pretty good, and depends especially on the radial resolution. The other two panels apply to a star rotating at 90% of the break-up rotation rate. Here the results are not as good. Evaluating the error in this case was not entirely straightforward due to difficulties in identifying the correct mode at different resolutions. The most likely cause for this decrease in accuracy is the presence of a cusp-like region at the equator which increases the resolution needed for calculating pulsation modes accurately.

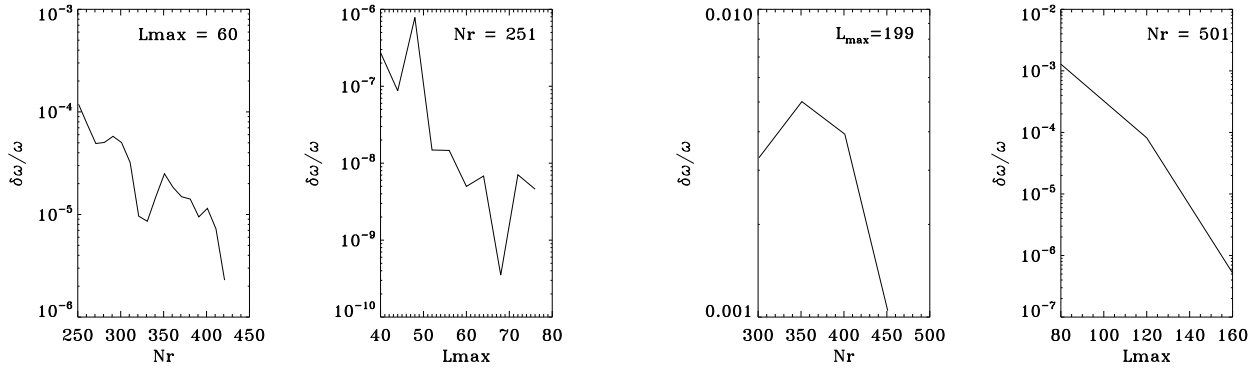


**Fig. 2.** Evolution of the error with $L_{\max}$ and $N_{\rm r}$ for a pulsation mode in a star at 60% of the break-up velocity (left two panels) and at 90% of the break-up velocity (right two panels).

Another test consists in applying a variational formula on the eigenmodes to yield an independent value for the frequency. According to the variational principle, the error on this frequency is proportional to the square of the error on the eigenmode, thus minimising its effect (Christensen-Dalsgaard & Mullan 1994). By comparing this value to the original frequency, it is possible to estimate the accuracy of the calculation. So far, we have only applied this test to pulsation modes in uniformly rotating models. For the pulsation mode which corresponds to the two left panels of Fig. 2, the relative error $\delta\omega/\omega$ is $2.5 \times 10^{-3}$ which corresponds to 0.7 $\mu$Hz. Unfortunately, the variational formula did not yield consistent values for the mode which corresponds to the two right panels.

Finally, another test consists in applying different numerical techniques to calculate the eigenmodes and seeing if they give similar results. Figure 3 shows such a comparison. The mode on the left is calculated using finite differences in the radial direction whereas the mode on the right uses Chebyshev polynomials. This second calculation required interpolating the stellar model onto the Chebyshev collocation grid using cubic splines in the same way as is done in Dintrans & Rieutord (2000) for a 1.5 $M_\odot$ CESAM model. At a given $L_{\max}$, the two calculations yield very similar results, as can be seen from the figure. The corresponding frequencies are less than 0.1 $\mu$Hz apart.

## 5 The results

Based on this method, we investigated pulsation modes in models with masses ranging from 1.7 to 25 $M_\odot$. The rotation profile for the models went from uniform to highly differential. The pulsation modes in uniformly or

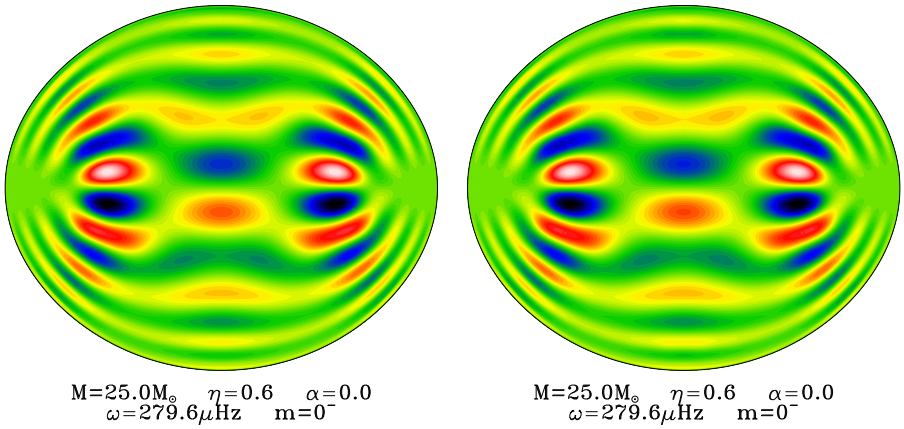


**Fig. 3.** Comparison of a pulsation mode calculated using finite differences (*left*) and using Chebyshev polynomial (*right*). The difference on the frequencies is less than 0.1 $\mu$Hz.

nearly uniformly rotating models followed the same qualitative behaviour as was found for polytropic models (Lignières et al. 2006; Reese et al. 2008a; Lignières & Georgeot 2008) in terms of mode geometry, mode classification and frequency organisation. Pulsation modes in the models with highly differential rotation turned out to be rather chaotic and difficult to classify. A more detailed discussion of these results is given in Reese et al. (2008b).

Many of the numerical calculations were carried out on the Altix 3700 of CALMIP ("CALcul en MIdi-Pyrénées") and on Iceberg (University of Sheffield), both of which are gratefully acknowledged. DR gratefully acknowledges support from the UK Science and Technology Facilities Council through grant ST/F501796/1, and from the European Helio- and Asteroseismology Network (HELAS), a major international collaboration funded by the European Commission's Sixth Framework Programme. The National Center for Atmospheric Research is sponsored by the National Science Foundation.

## References

Christensen-Dalsgaard, J. & Mullan, D. J. 1994, MNRAS, 270, 921

Dintrans, B. & Rieutord, M. 2000, A&A, 354, 86

Domiciano de Souza, A., Kervella, P., Jankov, S., et al. 2003, A&A, 407, L47

Espinosa, F., Pérez Hernández, F., & Roca Cortés, T. 2004, in ESA SP-559: SOHO 14 Helio- and Asteroseismology: Towards a Golden Future, 424–427

Jackson, S., MacGregor, K. B., & Skumanich, A. 2004, ApJ, 606, 1196

Jackson, S., MacGregor, K. B., & Skumanich, A. 2005, ApJS, 156, 245

Lignières, F. & Georgeot, B. 2008, Phys. Rev. E, 78, 016215

Lignières, F., Rieutord, M., & Reese, D. 2006, A&A, 455, 607

Lovekin, C. C. & Deupree, R. G. 2008, ApJ, 679, 1499

MacGregor, K. B., Jackson, S., Skumanich, A., & Metcalfe, T. S. 2007, ApJ, 663, 560

Ostriker, J. P. & Mark, J. W.-K. 1968, ApJ, 151, 1075

Reese, D., Lignières, F., & Rieutord, M. 2006, A&A, 455, 621

Reese, D., Lignières, F., & Rieutord, M. 2008a, A&A, 481, 449

Reese, D., MacGregor, K. B., Jackson, S., Skumanich, A., & Metcalfe, T. S. 2008b, in 38th Liège International Astrophysical Colloquium, in preparation

Rieutord, M. 2006, A&A, 451, 1025